Nigerian Journal of Physics (NJP)
ISSN online: 3027-0936
ISSN print: 1595-0611
DOI: https://doi.org/10.62292/njp.v35i4.2026.635
Volume 35(4), December 2026

A Study of Pre-Earthquake Ionospheric Anomaly (PEIA) in Low Latitude/ Equatorial Region TEC Using the Wavelet Power Spectrum Method

*[1,2]Kotoye, Afolabi Adegboyega, [2]Falayi, Olukayode Elijah, [2]Adepitan, Johnson Olufemi, [3]Adekoya, Bolarinwa John, [2]Adelaja, Ayobamidele Dele and [2]Bamidele, Kayode Johnson

[1]Abraham Adesanya Polytechnic, Ijebu Igbo, Nigeria
[2]Tai Solarin Federal University of Education, Ijagun, Nigeria
[3]Olabisi Onabanjo University, Ago-Iwoye, Nigeria

*Corresponding Author's Email: afobuddy@gmail.com

Keywords:
Earthquake,
TEC, WPS,
Low-latitude/equatorial region,
PEIA.

Submitted: 30 Jun. 2026

Accepted: 16 Jul. 2026

Published: 27 Jul. 2026

ABSTRACT

Earthquakes are major natural hazards that often result in significant loss of life and property. Previous studies indicate that the ionosphere exhibits anomalous behavior prior to seismic events. This study investigates pre-earthquake ionospheric anomalies (PEIA) associated with five earthquakes of magnitude M ≥ 7.0 in the low-latitude/equatorial region using Total Electron Content (TEC) data. Earthquake parameters were obtained from the United States Geological Survey (USGS), while TEC data were sourced from the International GNSS Service (IGS) via Ionolab, covering 10 days before and 5 days after each event. To distinguish seismic effects from external influences, geomagnetic and solar conditions were assessed using Dst, Kp, AE, and F10.7 indices from the OMNI database. Analysis using time series and Wavelet Power Spectrum (WPS) methods revealed significant TEC anomalies up to 10 days before each earthquake. WPS results further showed enhanced power intensity during the pre-earthquake period compared to quiet conditions. These findings demonstrate the role of lithosphere–atmosphere–ionosphere coupling mechanisms prior to major earthquakes, suggesting that PEIA is driven by multiple mechanisms.

INTRODUCTION

An earthquake is one of the most destructive natural disasters which cause high death tolls and large financial losses each year. Its occurrence is connected with the earth's crustal dynamics (Argunov and Gotovcev, 2021). The huge losses suffered by mankind shows that there is a great need to search for reliable earthquake precursors which will provide an advance warning of the coming disaster. Large earthquakes are often preceded or accompanied by signals of different natures such as variations in electric and magnetic fields and the generation and propagation of seismic waves, which are the most obvious manifestation (Argunov & Gotovcev, 2021; Draz et al., 2023). Recent advancements in earthquake (EQ) research and engineering have significantly enhanced our understanding of seismic hazards, fault mechanics, and early warning systems (Draz *et al.,* 2023; Lizunov *et al.,* 2020). Seismo-ionospheric studies is an emerging field of interest which aims to ultimately predict the occurrence of an earthquake by observing anomalous behaviors in the ionosphere within a period of about 1-10 days before an earthquake. While great care must be taken before concluding that the observed anomalies are related to the incoming earthquake because of the diurnal variation of the F2 layer , they might yet provide an insight into the coupling between the earth surface and the ionosphere (Anagnostopoulos, 2021). It is therefore clear that the existence of the ionospheric precursors of earthquake is still an open issue because firstly, it is difficult to isolate ionospheric anomalies of seismic origin from those from other drivers. Secondly, the physical mechanism of seismo-ionospheric coupling is not well understood. For these reasons, further observations to search ionospheric perturbations related to pre-earthquake seismic activity are urgently needed to shed light on the problem.

Xu *et al.,* (2022) studied the potential precursory pattern at Earth surface and the Ionosphere before two Mw ≥ 7 Earthquakes in Mexico in 2020–2021. In that study, thermal and ionospheric anomalies related to the Earthquakes (Mw ≥ 7.0) were investigated during 3 tidal force periods. It was concluded from the study that seismic thermal anomalies are strongly correlated with ionospheric perturbations. The research proves the existence of PEIA and also shows that its detection depends on proximity to the epicenter. In another study by Denisenko & Zeng, (2020), variations of TEC and foF2 as precursors to Earthquakes were analyzed for 4 Earthquakes which occurred in March 2018. The study confirmed the presence of PEIA and further showed that the greater the magnitude of the Earthquake, the higher the possibility of PEIA. Also, the deepest event observed had no effect on the ionosphere. However, the research studied 4 Earthquakes in close proximity thereby increasing the possibility of interference across the events. Also, since the events occurred during a mild storm, it is possible that the observed variations might be susceptible to forcing from the geomagnetic storm. Eshkuvatov *et al.,* (2023) studied ionospheric precursors of strong Earthquakes observed using six GNSS stations data over a period of five years (2011-2015). The results show continuous anomalous variations in TEC during 24 h before the local Earthquakes. The research proves the existence of PEIA but does not provide any explanation of the mechanism responsible. It also does not consider other ionospheric parameters like foF2. Shah *et al.,* (2020) studied possible ionospheric precursors related to Mw >6.0 Earthquakes in Japan using TEC and foF2 data. In that research work, PEIA was observed to occur within 5 days of an Earthquake. It was also observed that the location of maximum anomaly was not vertically above the epicenter, but southward. The study, however, was based on universal time instead of local time. This is of importance because Earthquakes are local events which have localized effects on the ionosphere. It is therefore important that associated variations must be reported in local time so as to eliminate the background diurnal variations in TEC. In this work, we have studied the anomalous variations in TEC within a period of 10 days before 5 major earthquakes with magnitudes ranging between 7.5 and 8.2. Both the time series method and the wavelet power spectrum (W.P.S) method were employed in order to establish the presence of PEIA and to reveal possible wave-like structures in the ionosphere during the pre-earthquake period. Considering the fact that many of the previous researchers had used the time series method to simply quantify anomalous variations in TEC, the W.P.S method is preferred due to its ability to reveal power concentration in TEC and wave-like features in the ionosphere. This is of immense benefit because observations from the W.P.S method may provide insight into the mechanisms responsible for the lithosphere-ionosphere-atmosphere coupling reported by previous researchers. To the best of our knowledge, none of the previous researchers has been able to clearly identify wave-like signatures, associated with forcing from below (lithospheric-atmospheric disturbance) during the PEIA period. Such signatures could be indicative of travelling ionospheric disturbances (TID), which is a consequence of the activities of atmospheric wave on ionospheric parameters

MATERIALS AND METHODS

For this study, 5 earthquake (EQ) events with magnitude *M*>= 7which occurred between 2015 and 2020 within the low-latitude region were identified as shown in Figure 1 below. A key factor which determined the choice of events to be studied was proximity to a G.P.S station. For example, events which took place in the sea or ocean were discarded for lack of TEC data. Information about earthquake events can be found at https://earthquake.usgs.gov/earthquakes. Such information includes the magnitude of the earthquake, depth, the epicenter, date and time. The list of earthquakes and their respective information is shown in Table 1.

Table 1: Showing earthquake related information

S/N	Event	Mag	Lat/Lon	Prep. Zone (km)	IGS Station	Lat/Lon	Dist. from epicenter (km)
1	Peru (2015)EQ	7.6	10.06S 71.01W	1,853	Arequipa	16.5S 71.5W	714
2	Solomon Island (2016) EQ	7.8	10.7S 161.327E	2,259.4	Vanuatu	17.74S 168.3E	1087
3	Mexico (2017) EQ	8.2	15.0N 93.9W	3357.4	Guatemala	14.6N 90.5W	366
4	Equador (2019) EQ	7.5	2.189S 77.1W	1678.8	Riobamba	1.65S 78.7W	187
5	Jamaica (2020) EQ	7.5	19.419N 78.8W	1678.8	Santiago de Cuba	20.01N 75.8W	320

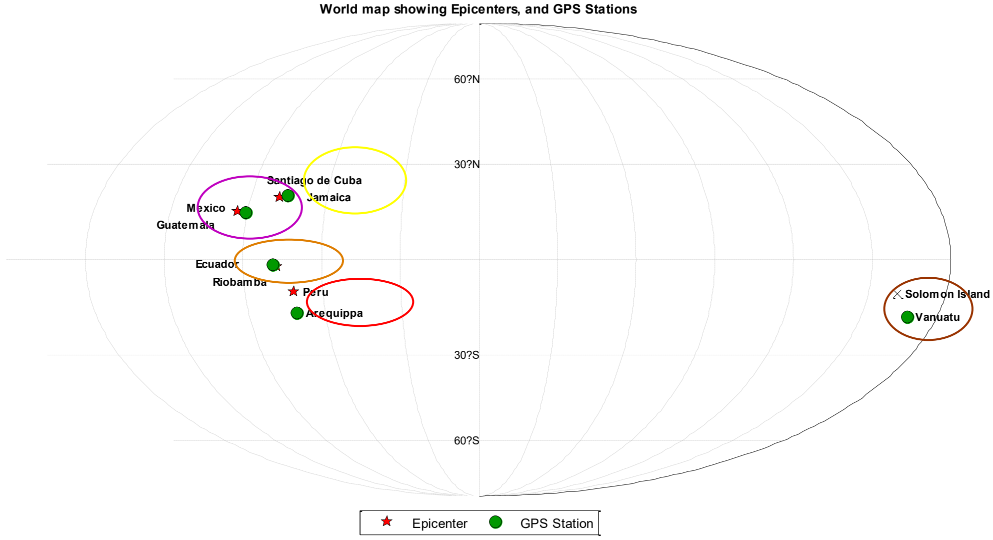

Figure 1: Map showing the positions of the epicenter and the GPS stations for each earthquake

In studying pre-Earthquake anomalies in the ionosphere arising from seismic origins, it is very important to separate variations due to solar and geomagnetic drivers from those caused by seismic activities. This involves specifying a set of criteria which can be used to separate disturbed days (geomagnetic and solar) from relatively undisturbed days 10-15 days before an earthquake. This gives a clear picture of the effects that an impending earthquake may have on the ionosphere. As a result, the undisturbed days are classified as those in which Dst > -25nT, Kp <2 and AE < 250nT (Mikhailov & Perrone, 2009; Patil et. al., 2016; Perrone et al., 2020; Chukwuma et al., 2021). Also, the enhancement/depletion must have an absolute value of *D(foF2)>20%* when considering the percentage deviation of TEC from the reference values. Lastly, the anomalous variation must be continuous for at least 2 hours (2 data points) during 10:00–18:00 LT. This will prevent the contributions from the sunrise effect, sunset effect and Q-disturbance.

Geomagnetic data used in this study consists of hourly values of the Dst index, the Kp index, the AE index and the f 10.7 index obtained from https://omniweb.gsfc.nasa.gov/cgi/nx1.cgi. For each event, TEC data was obtained from proximate GPS stations closest to the epicenter as illustrated in Figure 1. According to Xu Tong et al., 2010; Yao et al., 2012 and other researchers, in order to detect the possible anomalies in ionospheric parameters (in this case, TEC), the GPS station must fall within the preparation zone of the earthquake. This is estimated with the expression

$$P.Z = 10^{(0.43*M)} \quad (1)$$

where:

P.Z = preparation zone

M = Earthquake magnitude (Patil et. al., 2016).

GPS TEC data was obtained from the International Global Navigation Satellite Systems (GNSS) Service (IGS) at https://www.ionolab.org over a period of 10 days before each event and up to 5 days after. This gives a good view of the state of the ionosphere before, during and after an earthquake. Some works have reported greater days range, however, research has shown that PEIA is more prevalent between 7 and 10 days before an earthquake (Xu Tong et al., 2010; Chukwuma et al., 2021).

In this study, the bound method which was initially proposed by Liu et al., (2004) has been used to analyze data. TEC data has been plotted with upper and lower bounds as specified below:

$$\text{Upper bound (UB)} = X + 1.34\sigma \quad (2)$$

$$\text{Lower bound (LB)} = X - 1.34\sigma \quad (3)$$

where:

X is the data set

σ is the standard deviation

Assuming a normal distribution, the probability of TEC being within the interval between UB and LB is given as 85% (Xu et al. 2015; Patil et. al., 2016). If the value of TEC falls outside the bounds, there is a 90 – 95% confidence level that a lower or upper anomalous variation has been detected (Patil et. al., 2016). Furthermore, the method of estimating the percentage deviation of TEC from its reference values (quiet day values) has been used to qualitatively assess the anomalous variations (Liu, 2008; Chukwuma et al., 2021). It is expressed as:

$$D(f_0F2) = \frac{f_0F2 - (f_0F2)_Q}{(f_0F2)_Q} X\,100 \quad (4)$$

where:

$(TEC)_Q$ and $(f_0F2)_Q$ are quiet day values of both TEC and f_0F2 respectively.

In this method, following the example of Liu et al., (2008), Buresova & Lastovicka (2007) and Chukwuma et al., (2021), only anomalous variations with values of $D(f_0F2)$>20%, continuous over at least 2 hours between 12:00LT and 18:00LT were considered.

The Wavelet Power Spectrum (WPS) method, which provides great details about the transient variabilities in ionospheric parameters was used to analyse TEC data. WPS is a very effective mathematical tool for evaluating time series with different scales. This analysis technique offers information about the frequency of the event relative to its locality in the time series (Falayi et al., 2020). The WPS is created by the amplification, ψ(t)→ψ(t), and translations, ψ(t)→ψ(t+ 1), with reference to time t. The mother wavelet is presented in Equation (5)

$$?_{a,b}(t) = a^{\frac{1}{2}}?(\frac{t-b}{a}) \quad (5)$$

$$?(t) = \frac{e^{iw_0 t}}{\sqrt[4]{pe^{\frac{i^2}{2}}}} \quad (6)$$

$$\mathrm{WPS(a,b)} = \int_{-8}^{8} \mathrm{x(t)}\, ?^{*}_{\mathrm{a,b}}(t)dt \quad (7)$$

where:

$?_{a,b}(t)$ is the wavelength function

w_0 is the dimensionless frequency

$?^{*}_{\mathrm{a,b}}(t)$ is the conjugate of the wavelength function $?_{a,b}(t)$

t is the time

The expression of the wavelength coefficient at time index 'n' and scale 'a' is given as

$$\mathrm{WPS_n(a)} = ?_{\mathrm{n'=0}}^{\mathrm{N-1}}\, \mathrm{x(n)'}?*\,[\frac{(n'-n)dt}{a}] \quad (8)$$

Where N is the length of the data time series and dt represents the time interval. The scale-averaged WPS is used to examine variation in power over a band of scales as shown in equation (9)

$$\overline{\mathrm{W_n^2}} = \frac{?j?t}{0.776}\int_{j1}^{j2} \frac{|W(a_j)^2|}{a_j} \quad (9)$$

Upon analysis, a considerable energy distribution was perceived in TEC. Equations (5) - (9) were used to obtain the wavelet power spectrum analysis to estimate the time-frequency characteristics as shown in Figures 2 - 6.

RESULTS AND DISCUSSION

Figures (2, 5, 8, 11 and 14) show the daily variations of the Kp index, the Dst index and the AE index before each of the 5 EQ events studied respectively The Kp index is a standardized 0-to-9 scale that measures disturbances in the Earth's magnetic field caused by solar winds. Higher numbers indicate stronger geomagnetic storms, which directly affect the brightness and extent of the Northern and Southern auroras. A Kp index of 0 – 2 (Quiet) indicates little to no geomagnetic activity, hence, the Kp index threshold is given as Kp <2. The Dst index is a major indicator of geomagnetic disturbance in the ionosphere. It is a measure of the energy transfer from the incoming solar wind to the ring current within the magnetosphere (Sugiura 1963). The threshold for the Dst index is Dst > -25nT. The auroral electrojet (AE) Index is a measure of global geomagnetic activity in the auroral zones. It tracks the intensity of ionospheric currents (electrojets) caused by solar wind and magnetospheric storms. Higher values indicate greater space weather disturbance. The threshold for the AE index is AE < 250nT.

Figures (3, 6, 9, 12 and 15) present the plots of TEC variations, respectively, for all the EQ events studied. In the top panel of each figure, the red, black and green curves represent the observed *TEC*, the upper and lower bounds respectively. The lower panel presents the time series plot of *D*(*foF2*), with the broken horizontal lines representing the *D*(*foF2*) threshold value of 20%. The lower panel in all the figures show the results of the observation of pre-earthquake ionospheric anomalies. According to Liu et al. (2006), if the *foF2* variations are seismosensitive, the probability of observing the abnormal signals before earthquakes should be significant. Therefore, this research only considered precursor enhancement/depletion with an absolute value of *D*(*foF2)* > 20% continuous at least for 2 h (2 consecutive data points) during 12:00–18:00LT (Burešová & Laštovicka 2007; Liu et al. 2000, 2006, 2008). Also, figures (4, 7, 10, 13, 16) show the plots of the wavelet power spectrum for all thr events studied. The top panel is the plot for the PEIA period, while the lower panel is the plot for the reference (quiet) period. This comparism between quiet period and PEIA period is made so as to highlight the possible differences in power spectrum between both periods.

Peru (2015) Earthquake

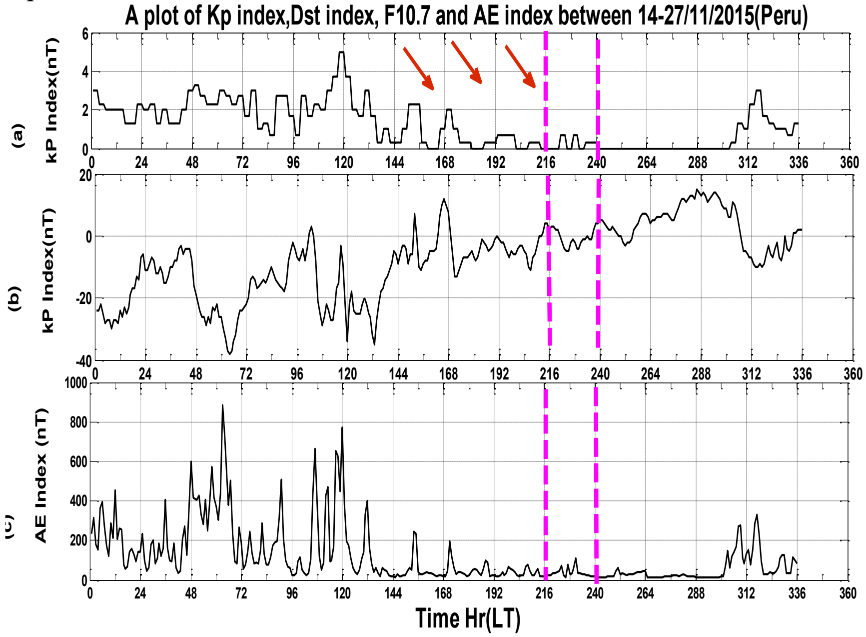

Figure 2: Geomagnetic indices for 10 days before and 5 days after the Peru EQ of 24th of Nov., 2015

Figure 2 presents the daily variation for the geomagnetic and solar indices for ten (10) days before the EQ (November, 14-23, 2015). The vertical lines indicate the earthquake day, (November 24, 2015). As shown in the figure, the plot for kp index was < 2nT on November, 23-25, 2015. Also, the Dst index was $Dst > -25$ nT within the same period, indicating a quiet geomagnetic condition. The AE index in the lower panel is also low (<250nT) within that period. A careful combinationof these indices reveal that November, 23-25, 2015 were indeed geomagnetically quiet days. Thus, any observed anomalous variation in TEC may be solely attributed to the impending earthquake event.

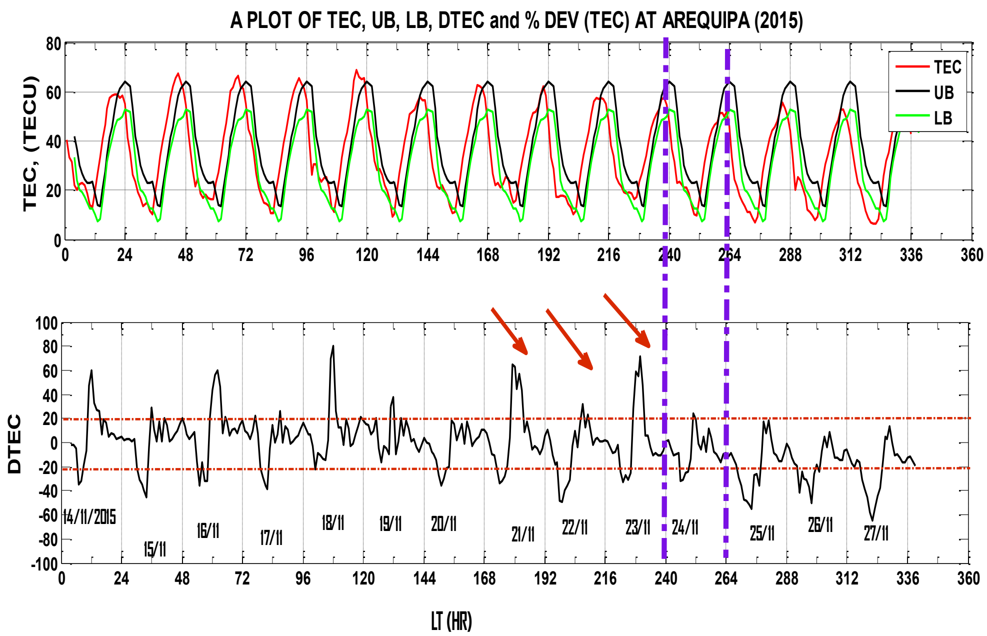

Figure 3: TEC variation at Arequippa GPS station during the Peru EQ of 24th of Nov., 2015. The top panel shows the observed TEC, upper and lower bounds while the lower panel shows the percentage deviation of the observed TEC from the upper and lower bounds. The arrows indicate quiet PEIA days, while the vertical lines indicate the earthquake day

From Figure 3, anomalous TEC enhancements were observed from days 1-3 (21/11-23/11,2015) before the EQ. The 21st of November recorded enhancement in TEC with a value of 57% to 43% between 10:00 LT and 11:00 LT. The anomalous variation observed on the 22nd of November cannot be reckoned with, since it lasts only for one hour. However, on the 23rd of November, variability ranged between 71% at 10:00LT and 47% at 11:00 LT.

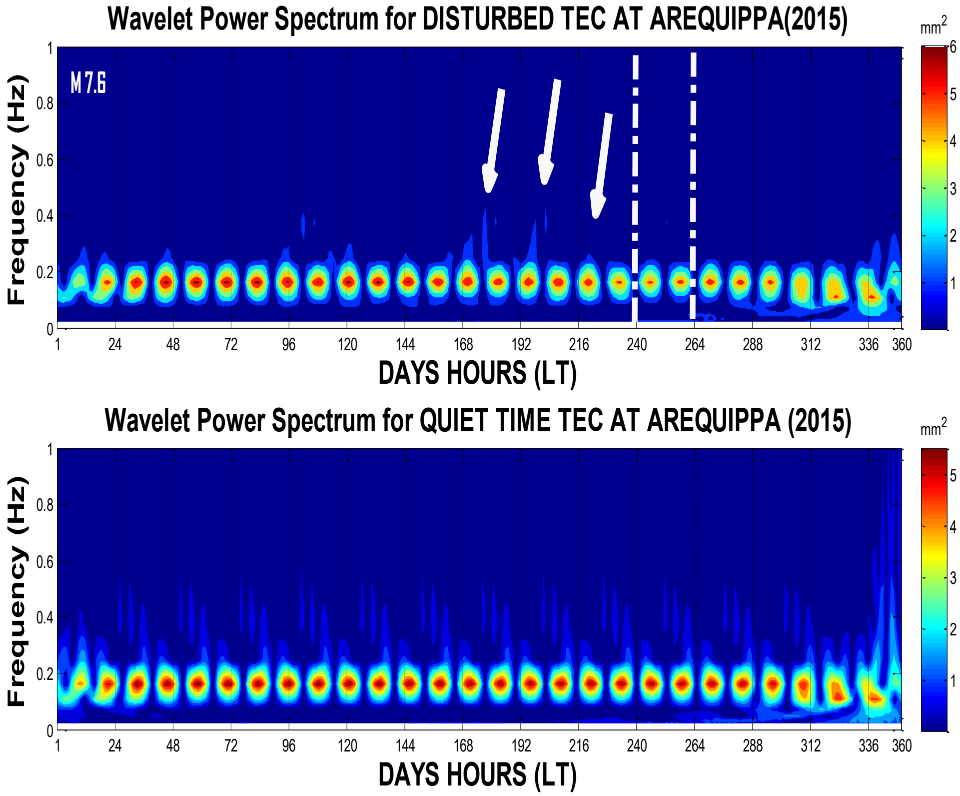

Figure 4: W.P.S of TEC at Arequippa

Figure 4 shows the WPS plot of the same event under review. The upper panel shows the WPS plot for the PEIA period, while the lower panel shows the same plot for the quiet period.

For the quiet-time TEC,the spectrum shows a highly regular sequence of repeating power maxima at the dominant diurnal scale.The power distribution is fairly uniform and there are no obvious isolated high-power events. During the PEIA period (Disturbed TEC), the repeating diurnal structure is still present, but several localized enhancements appear before the earthquake marker. These appear as transient features that are stronger than the surrounding background. The disturbance appears concentrated in time rather than extending across the entire period. Compared with the quiet case, the disturbed WPS contains additional transient energy superimposed on the regular daily cycle. The background periodicity is preserved, but the localized enhancements suggest a temporary modification of the TEC dynamics rather than a wholesale change in the dominant oscillation.

Solomon Island (2016) EQ

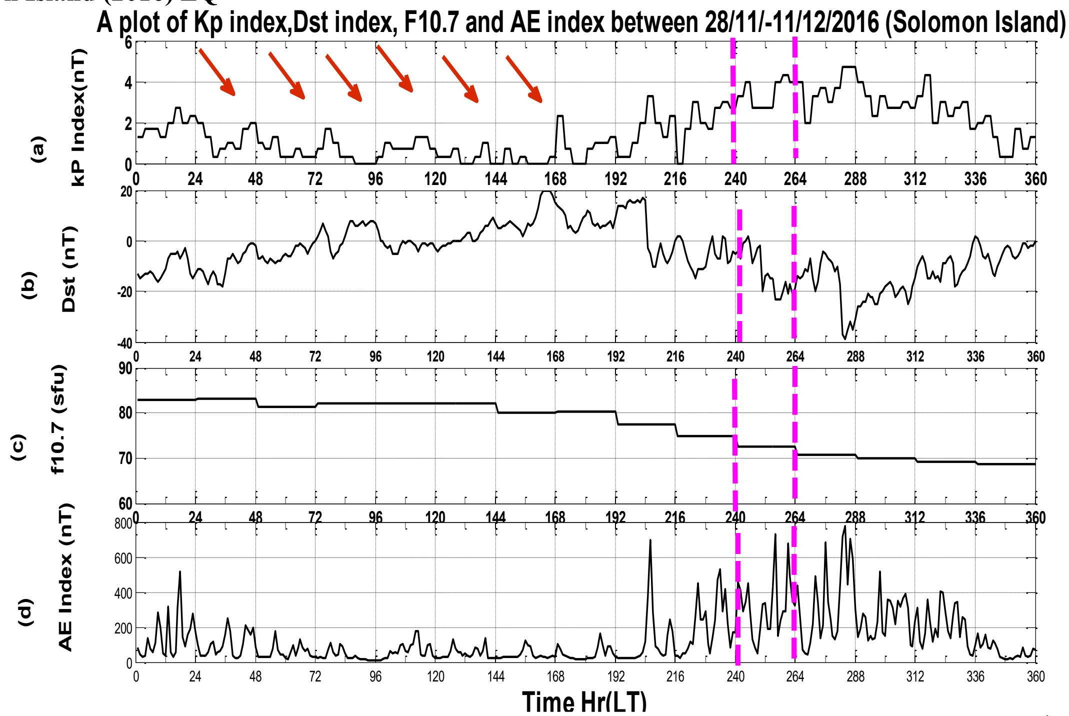

Figure 5: Geomagnetic indices for 10 days before and 5 days after the Solomon Island EQ of 8th of Dec., 2016

Figure 5 presents the daily variation for the geomagnetic and solar indices for ten (10) days before the EQ (28th of November - 7th of December, 2016). The vertical lines indicate the earthquake day, (8th of December, 2016). As shown in the figure, the criteria for kp index was < 2nT between the 30th of November and 4th of December, 2016. Also, the Dst index was *Dst*>−25 nT within the same period, indicating a quiet geomagnetic condition. The AE index in the lower panel is also low (<250nT) within that period. A careful combinationof these indices reveal that November, 23-25, 2015 were indeed geomagnetically quiet days. Thus, any observed anomalous variation in TEC may be solely attributed to the impending earthquake event.

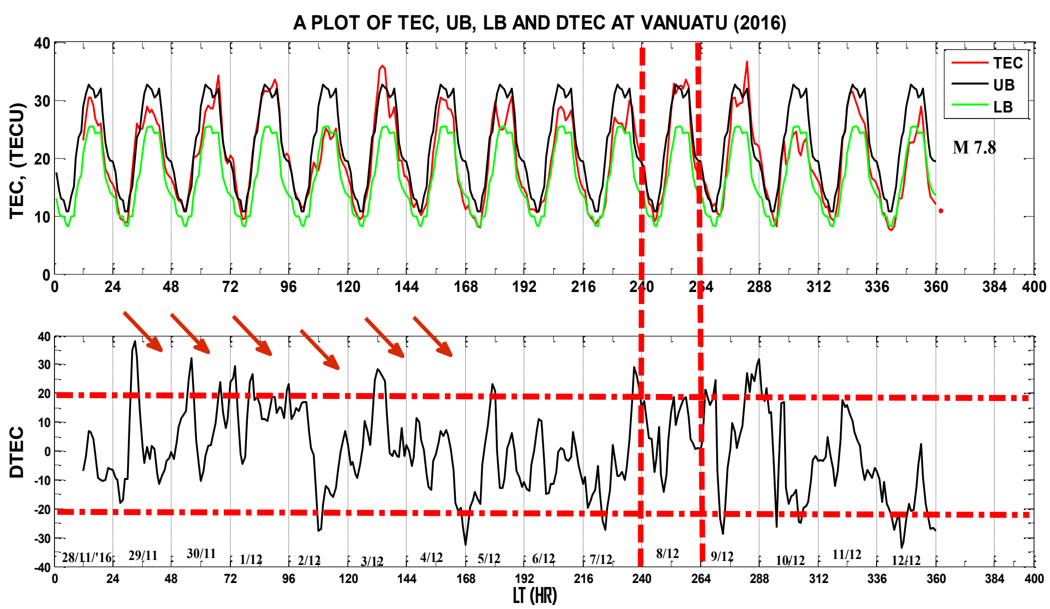

Figure 6: Same as Fig. 3, but for TEC variation at Vanuatu

As shown in the lower panel, there was significant variation in TEC during the day time hours on days 5 to 9 (29/11 to 3/12/2016). On day 6 (2/12/2016), a depletion was recorded between 12:00LT and 14:00 LT with values ranging between -28% and -25%. whereas, the other days experiences an enhancement. Even though day 4 (4/12/2016) was identified as a possible precursor day, no significant enhancement or depletion was recorded.

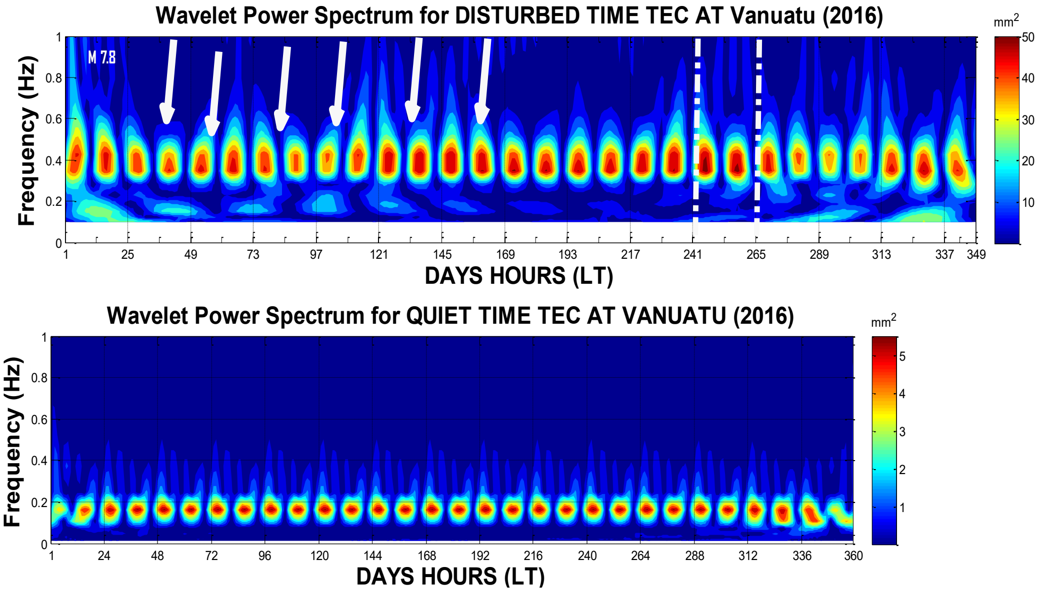

Figure 7: WPS of TEC at Vanuatu

Figure 7 shows the WPS plot of the same event under review. The upper panel shows the WPS plot for the PEIA period, while the lower panel shows the same plot for the quiet period. During the quiet-time, TEC displays a consistent pattern of regularly spaced power peaks associated with the diurnal variation. The spectrum is visually homogeneous with little evidence of isolated anomalies.However, during the PEIA period,the spectrum exhibits much stronger power intensity than the quiet spectrum. This is reflected by the substantially larger color-scale range.High-power regions occupy a broader portion of the spectrum and are more persistent through time.While the diurnal oscillation remains visible,it is however embedded within a stronger background of wavelet power. Among all the stations considered, Vanuatu presents one of the clearest contrasts between disturbed and quiet conditions. The earthquake-period spectrum is characterized by a marked amplification of power while retaining the underlying periodic structure. This suggests an increase in oscillation amplitude rather than disappearance of the dominant periodicity.

Mexico 2017 Earthquake

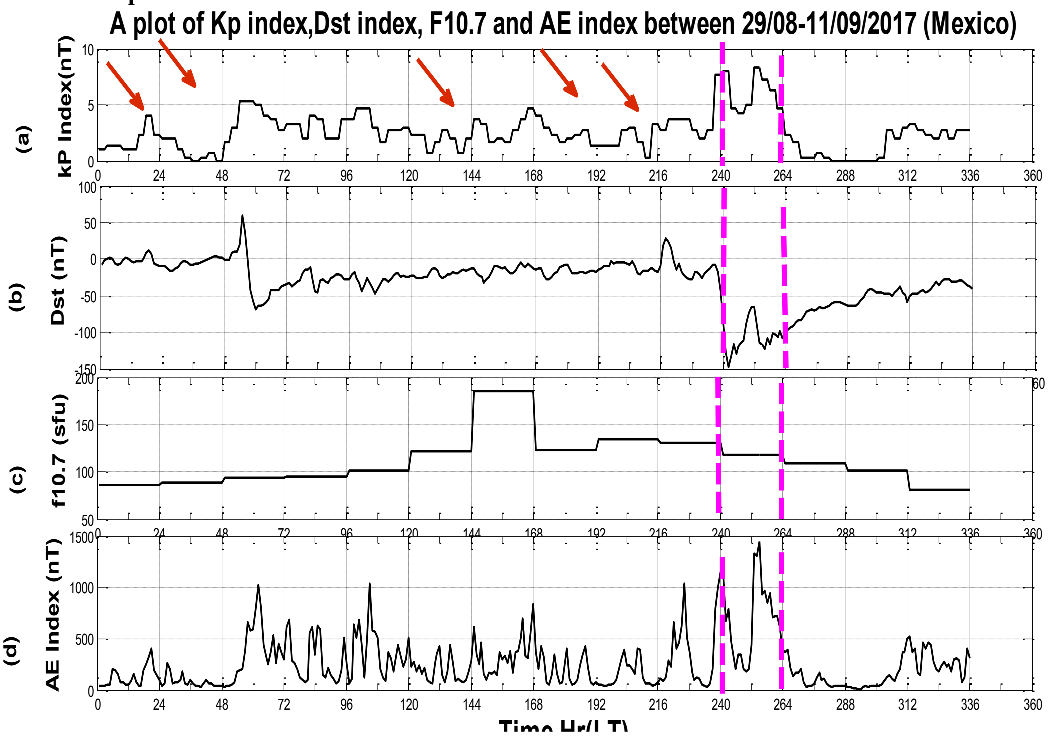

Figure 8: Geomagnetic indices for 10 days before and 4 days after the Mexico EQ of 8th of Sept., 2017

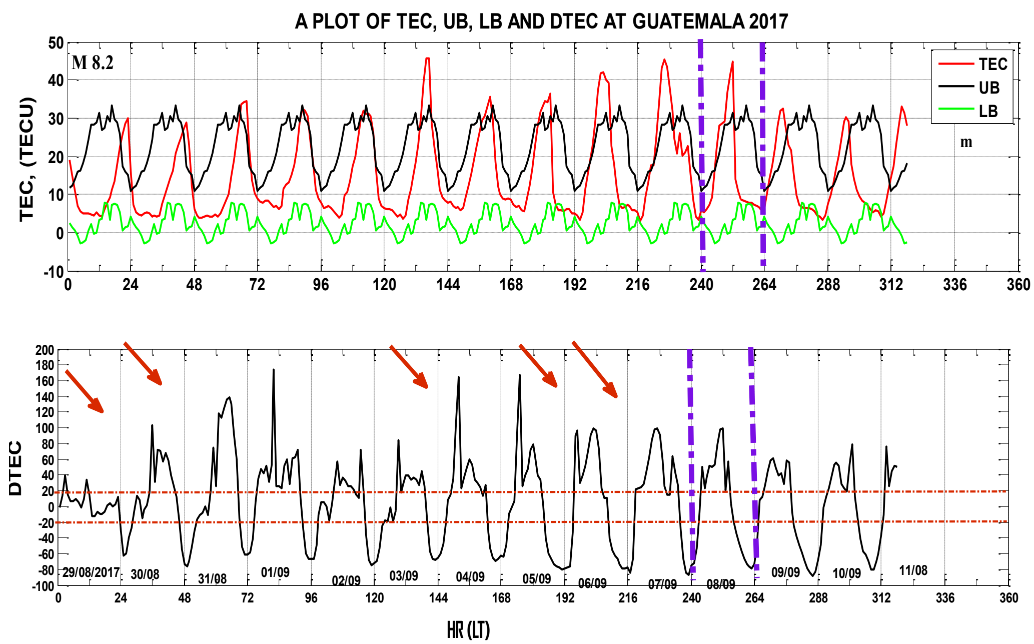

Figure 9: Same as Fig. 3, but for TEC variation at Guatemala

As shown in the lower panel, days 2, 3,5,9 and 10 are identified as possible presurssor days. On day 2 (06/09/2017), enhancement ranged between 99.17% at 10:00LT and 73.7% at 12:00LT. A depletion ranging from -40.6% to -62.09% was also recorded between 16:00LT and 18:00LT. Day 3 (05/09/2017) also recorded anomnalous enhancement and depletion during the day. Days 5 and 9 (03/09/2017 and 30/08/2017) experience anomalous expansion during daytime hours. Day 10 (29/08/2017) does not record any anomalous behavior because the enhancement is not continous for up to 2 hours.

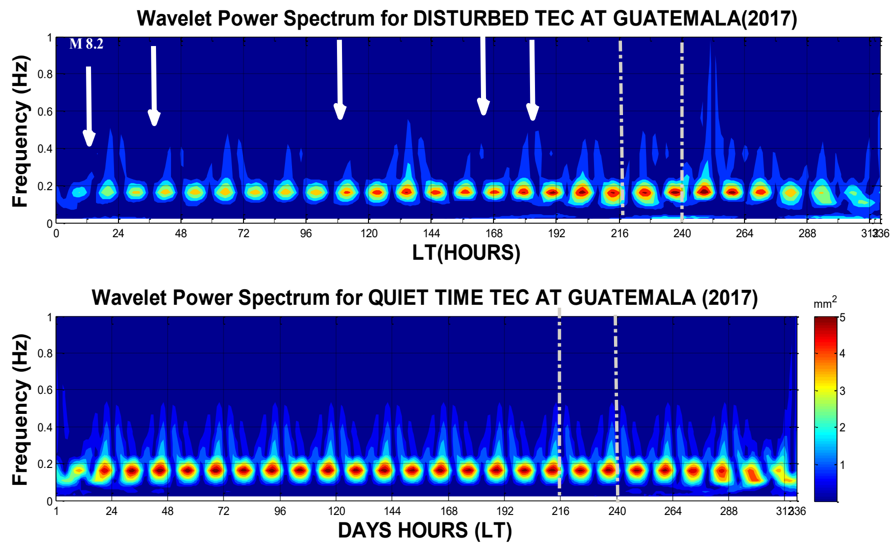

Figure 10: WPS of TEC at Guatemala

The plot of the quiet-time TEC shows a stable and repeating sequence of diurnal power maxima.Energy remains concentrated near the principal periodic component with relatively little temporal variability.The disturbed TEC reveals localized increases in wavelet power, which interrupt the otherwise regular diurnal TEC pattern.The anomalies are both temporal and confined rather than continuous.Relative to the quiet spectrum, the disturbed case demonstrates additional intermittent activity while preserving the dominant daily cycle. The principal difference lies in the appearance of localized power bursts rather than a shift in the dominant frequency content.

Ecuador EQ 2019

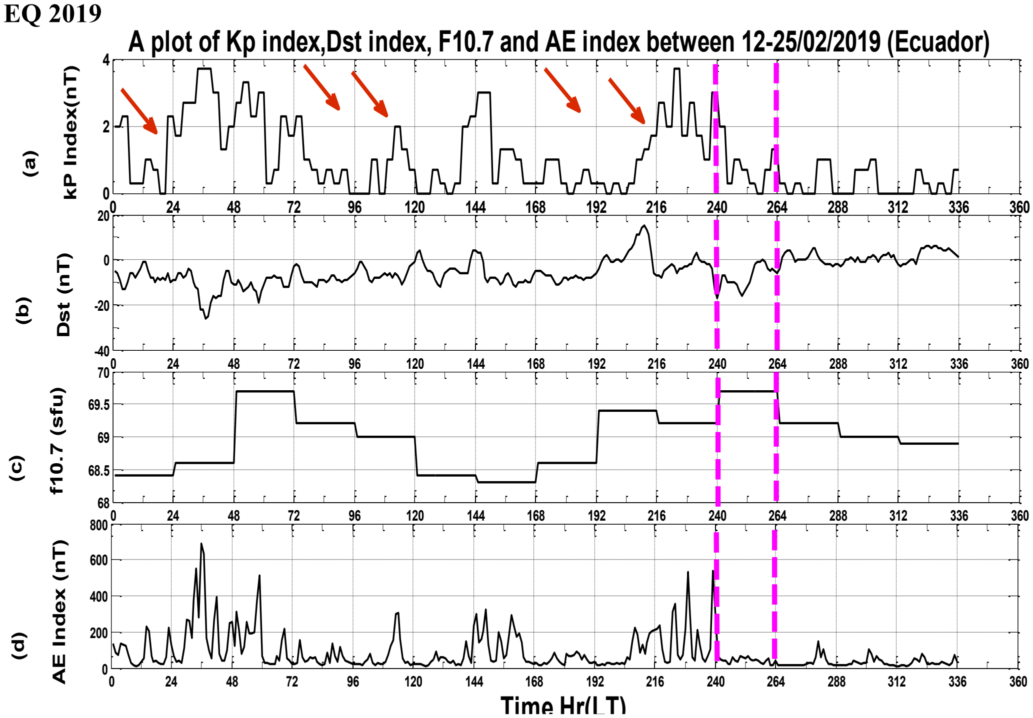

Figure 11: Geomagnetic indices for 10 days before and 5 days after the Ecuador EQ of 22nd of Feb., 2019

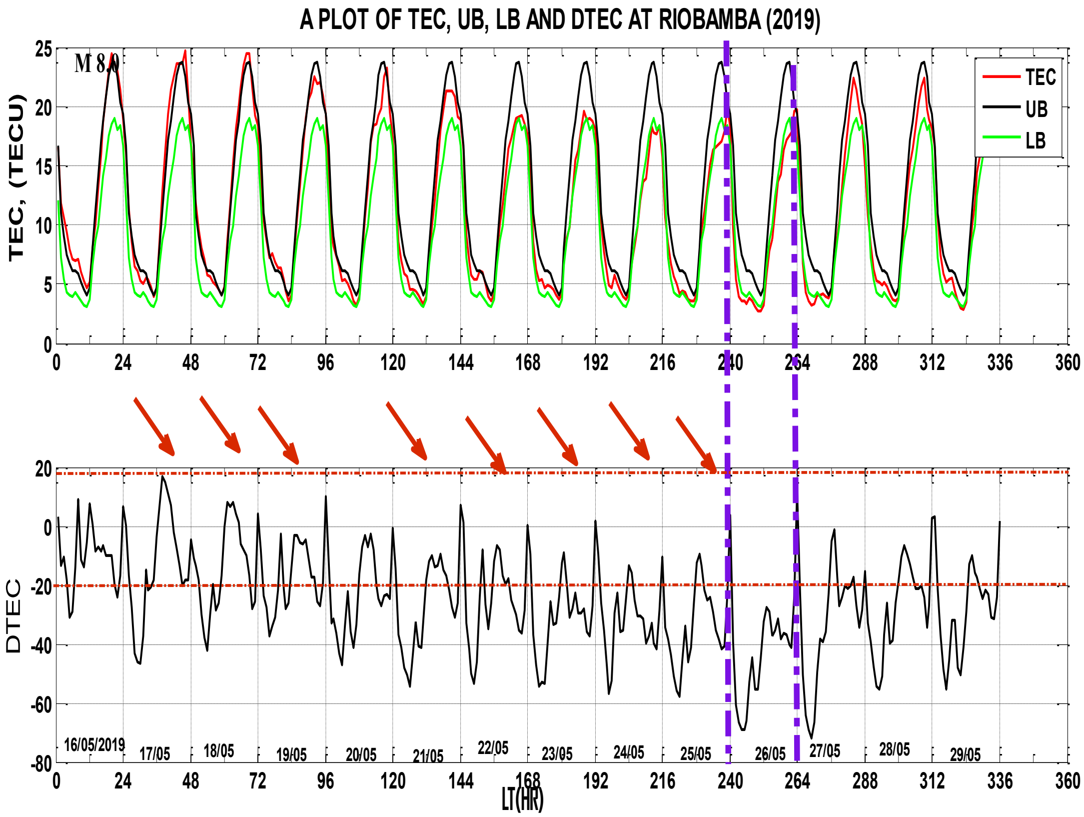

Figure 12: Same as Fig. 3, but for TEC variation at Riobamba

As shown in Figure 12, no anomalous variation was observed on days 2 – 4 (18- 20/02/2019) and 7 – 9 (13-15/02/2019). On days 5 and 6 (16-17/02/2019), enhancement was recorded between 12:00 LT and 14:00LT, while on day 10 (12/02/2019), a slight depletion was also recorded.

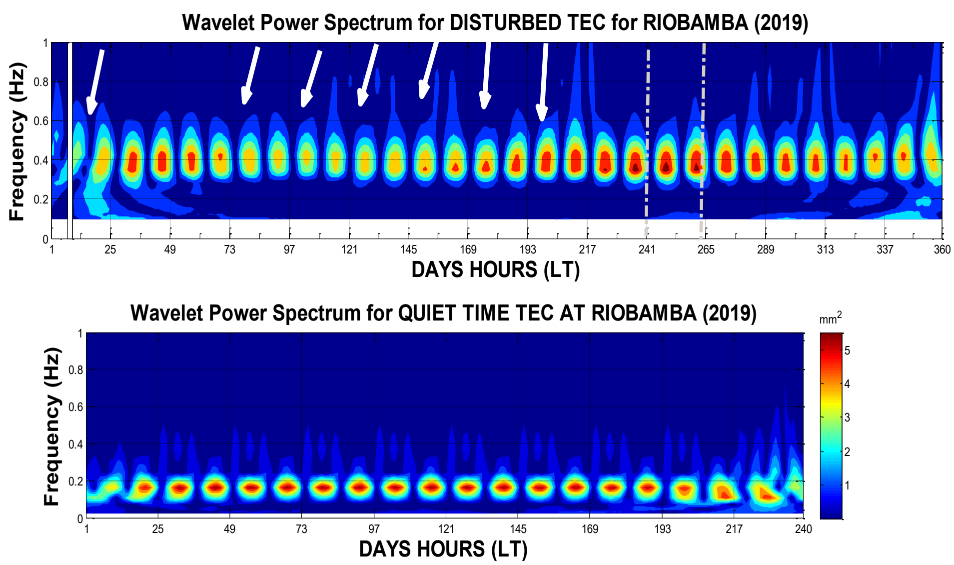

Figure 13: WPS for TEC at Riobamba

Figure 13 shows the plots for both PEIA period and quiet time TEC as observed at Riobamba prior to the February, 2019 EQ in Ecuador. The quiet time spectrum reveals a highly regular signature with nearly identical repeating power maxima across the period considered. There is little visual evidence of abrupt spectral changes in the figure.The PEIA time TEC reveals a particularly strong power concentration. The spectrum shows enhanced activity relative to the quiet period, especially during the earlier portion of the observation window. Despite the enhanced activity during the disturbed period, the background diurnal signature of TEC remains identifiable. The major difference between the disturbed time TEC and the quiet time TEC is the strong enhancement in wavelet power in the early stages of the disturbed period. This indicates that the disturbance is localized in time rather than persistent throughout the observation period.

Jamaica EQ (2020)

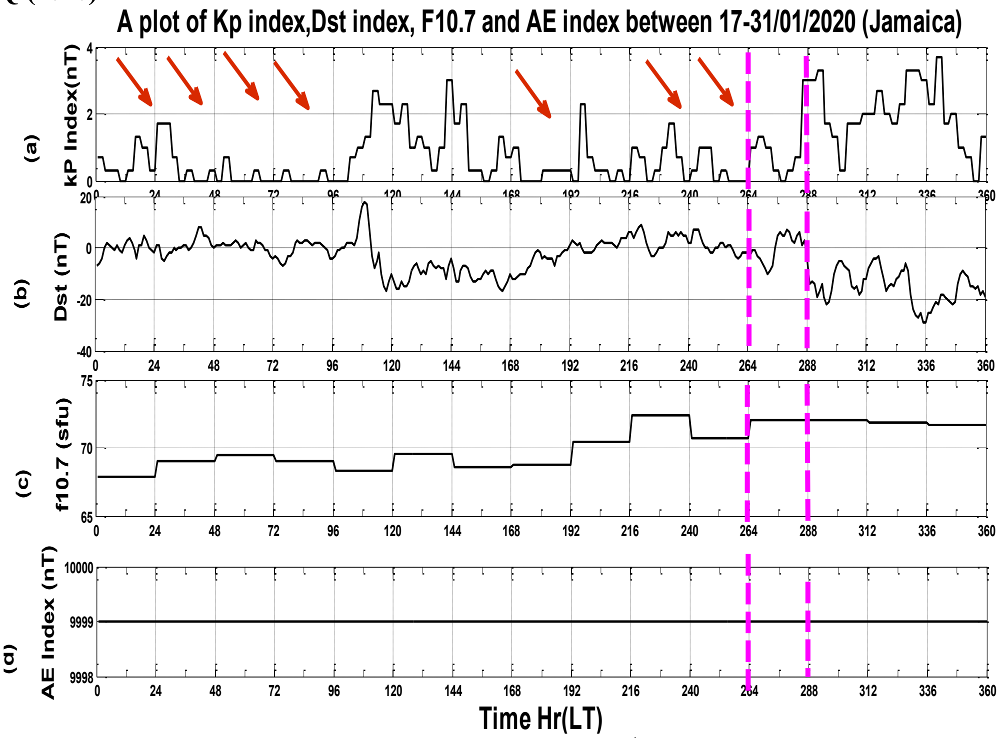

Figure 14: Geomagnetic indices for the Jamaica EQ of 28th of Jan., 2020

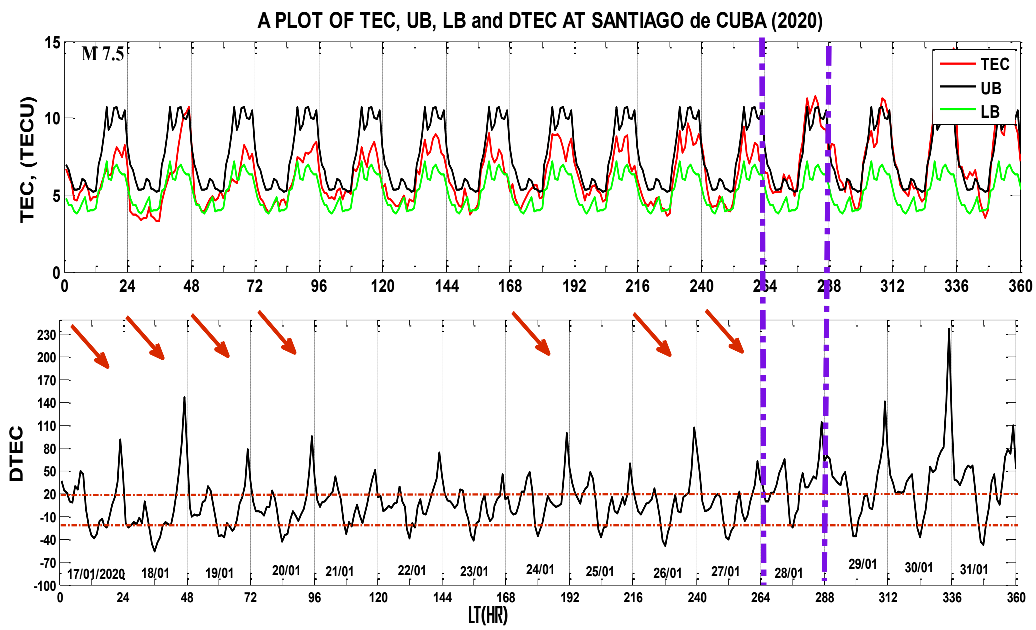

Figure 15: Same as Fig. 3, but for TEC variation at Santiago de Cuba

Figure 15 shows the plot of TEC during the PEIA period before the Jamaica EQ of 28/01/2020.
As shown in the lower panel, days 1, 2, 4,8,9 and 10 are identified as possible precursor days. On days 1, 2 and 4 (27,26 and 25 /01/2020), anomalous depletion is observed between 11:00LT and 13:00LT. A similar depletion is observed on days 8 - 10 (20/01/2020 - 18/01/2020). Those depletions occurred during daytime hours.

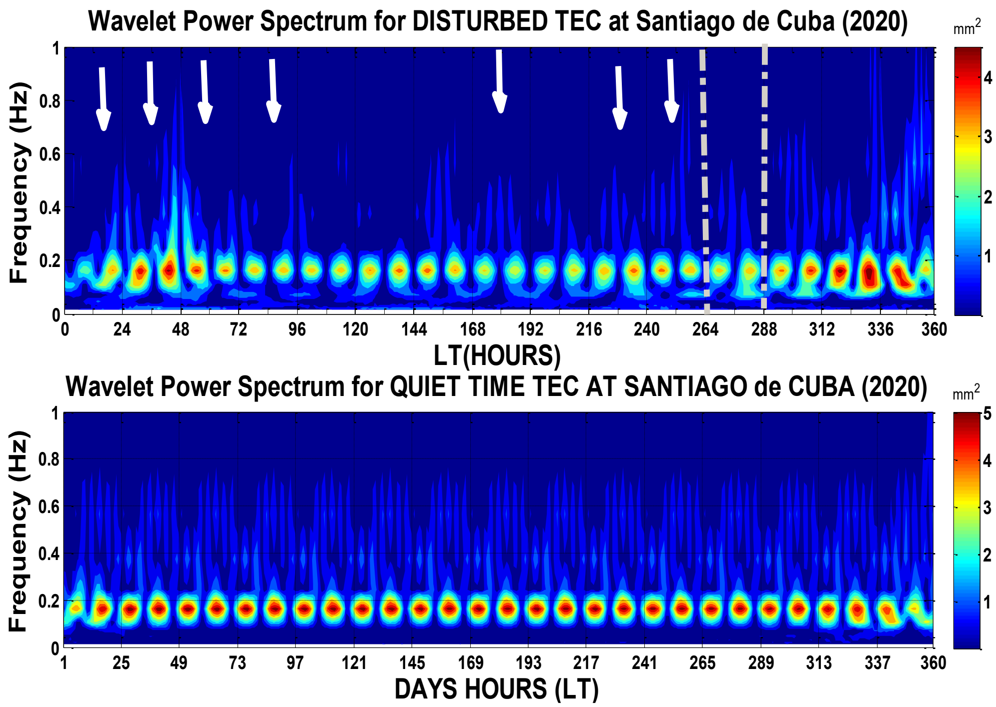

Figure 16: WPS for TEC at Santiago de Cuba

Figure 16 shows the WPS plot for both quiet-time and disturbed-time TEC. During the quiet period, TEC exhibits a regular diurnal pattern with nearly uniform peak amplitudes. Thus, spectral power remains relatively stable over the observation interval.During the disturbed period, the spectrum reveals several conspicuous localized enhancements which occur while the underlying daily oscillation continues to be visible. From the plot, it can be seen that the power distribution is more uneven than during the quiet period. Compared with quiet conditions, TEC during the disturbed period displays increased temporal variability and isolated power enhancements without eliminating the dominant periodic behavior. The anomalies therefore appear as transient modifications of an otherwise persistent daily cycle.
As mentioned earlier, the search for PEIA requires a careful approach and stringent measures. This is to ensure that the effect of forcing from solar and geomagnetic events are separated from those from seismic origin. The results shown in figures 3,6,9,12 and 15 show anomalous enhancement/depletion across all the cases considered. Enhancements were observed at Arequippa, Vanuatu, Guatemala and Riobamba while depletion was only observed at Santiago de Cuba. All these results suggest that there might exist a coupling mechanism between the lithosphere and the ionosphere.
The quiet-time WPS plots are characterized by stable and persistent diurnal TEC oscillations with relatively uniform power distributions. During earthquake-associated intervals, the dominant daily periodicity is generally preserved, but additional localized wavelet power enhancements and increased temporal variability become evident. The magnitude of these changes varies by event, with Vanuatu displaying the strongest overall amplification and other stations exhibiting more localized transient anomalies. These observations are consistent with temporary perturbations superimposed on the background solar-driven ionospheric dynamics rather than a replacement of the underlying periodic structure. This implies that these enhancements are intermittent and time-localized, indicating temporary injections of energy into the ionosphere. The ionosphere remained primarily controlled by regular solar-driven processes, but experienced additional disturbances during the PEIA interval that temporarily increased the amplitude or complexity of TEC fluctuations. The results obtained suggest that there is a seismo-ionospheric coupling in the days leading to an EQ. The proposed mechanisms include radon emission and atmospheric ionization coupled with

latent heat release, changes in atmospheric conductivity, magnetospheric particle precipitation and acoustic-gravity wave generation. Previous researchers had attempted to explain the observed anomalous seismo-ionospheric variations. Namgaladze et al.(2009b) proposed that the probable reason for electron density disturbances before earthquake is the vertical drift of the F2-region ionospheric plasma under the influence of the zonal electric field of seismic origin. The vertical upward electromagnetic drift in the mid-latitude, created by eastward electric field, leads to the increase in electron density while the westward electric field creates the depletion effect in TEC. Zolotov et al. (2012a & b) also related the observed anomalies to the electromagnetic effect of the lithosphere-atmosphere–ionosphere coupling (LAIC) mechanism. Pulinets & Boyarchuk,(2004) proposed that the vertical seismogenic field mechanisms generated at the preparation zone of the seismic event penetrate the ionosphere and create the observed irregularities in electron concentration.

While the enhancements and depletions observed in this study can be explained by plasma drift under the influence of zonal electric field as proposed by Namgaladze et al.,(2009b), the transient spectral enhancements are consistent with perturbations that could arise from Travelling Ionospheric Disturbances (TID). Such disturbances are known to emanate from Atmospheric Gravity Waves (AGWs) or related upward-propagating disturbances (Jonah et al., 2016, 2020; MacDougall & Jayachandran, 2011). TIDs are the signatures of AGWs in the ionosphere.When a disturbance occurs in the lower or upper atmosphere, it creates an oscillating wave. As this wave travels upward into the extremely thin air of the ionosphere, it pushes and pulls the charged plasma, creating moving "crests" and "troughs" of electron density (Jonah et al., 2016, 2020; Habarulema et al., 2018). The intermittent and time-localized features revealed by the WPS can hence be attributed to short bursts of upward-propagating disturbances of seismic origin. Considering the results from the time series plots and the WPS, it is evident that a single mechanism might not suffice in explaining the lithosphere-atmosphere-ionosphere coupling effect (LAIC). This is in contrast to the explanations proposed by previous researchers. For example, in their study of the Tohoku EQ event, Chukuma et al., (2021) had identified magnetospheric plasma precipitation as the only driving mechanism for LAIC. Pulinets & Boyarchuk, (2004) had proposed that the vertical seismogenic electric field generated within the preparation zone penetrates the ionosphere, causing the observed irregularities. The same view is held by Kim et al., (1994) and Pulinets et al., (2000). However, while studying the abnormal perturbations in the ionospheric F2 region before the Wenchuan earthquake, Kelley et al., (2017) dismissed the possibility of electric field and AGW of seismic sources reaching up to ionospheric heights to cause pertubations in TEC. They proposed that the positive perturbations observed on a precursor day could be pre-determined by the thermosphere-ionosphere system in the sunset hours of the previous day under the influence of the impending earthquake.

CONCLUSION

The results of this study revealed significant enhancement/depletion up to 10 days prior to major earthquakes. This shows that detection and justification of the existence of pre-earthquake ionospheric precursors can be achieved by a set of requisite criteria that indeed differentiates ionospheric precursors of seismic origin from those from other sources.

Wavelet power spectrum analysis revealed that the dominant diurnal TEC oscillation persisted during both quiet and pre-earthquake intervals, indicating continued control by solar-driven ionospheric processes. However, the pre-earthquake periods exhibited localized enhancements in wavelet power and increased temporal variability, suggesting the presence of transient disturbances superimposed on the background state. These spectral changes are consistent with perturbations that may be associated with upward-propagating atmospheric gravity waves and / or acoustic-gravity waves. Similarly, the observed spectral changes could be related to lithosphere–atmosphere–ionosphere coupling mechanisms of electric and magnetic origin. Examples of such coupling mechanism include variations in seismogenic electric and magnetic field strength. While the present analysis does not uniquely distinguish among these mechanisms, it demonstrates that the ionosphere's response to an impending EQ cannot be adequately explained by a single mechanism; rather, the coupling process is a combination of mechanisms, both mechanical and electromagnetic of seismic origin. More studies (both observational and modelling) are required to identify the particular upward propagating wave that is responsible for the wave-like signature found in the ionosphere in the build-up to a major EQ.

ACKNOWLEDGEMENT

The authors wish to thank the International GNSS Service (IGS) and the National Aeronauticsa and Space Administration (NASA) for supplying GPS and earthquake data respectively.

REFERENCES

Anagnostopoulos, G. (2021). On the origin of ULF magnetic waves before the Taiwan Chi-Chi 1999 earthquake. Frontiers in Earth Science, 9, 730162.

Argunov, V. V., & Gotovcev, M. R. (2021). Study of ionospheric effects and earthquake precursors using radio engineering methods. IOP Conference Series: Earth and

Environmental Science, 720(1), 012087. https://doi.org/10.1088/1755-1315/720/1/012087

Burešová, D., & Laštovička, J. (2007). Pre-storm enhancements of foF2 above Europe. Advances in Space Research, 39(8), 1298–1303. https://doi.org/10.1016/j.asr.2007.03.003

Chukwuma, V. U., et al. (2021). On the significance of requisite criteria in detecting pre-earthquake ionospheric precursors. Acta Geophysica, 69, 1545–1566.

Denisenko, A., & Zeng, Z. (2020). The analysis of earthquake precursors in variations of TEC in the ionosphere and the subsequent impact on the environment. IOP Conference Series: Earth and Environmental Science, 421(2), 022034. https://doi.org/10.1088/1755-1315/421/2/022034

Draz, M. U., Shah, M., Jamjareegulgarn, P., Shahzad, R., Hasan, A. M., & Ghamry, N. A. (2023). Deep machine learning–based possible atmospheric and ionospheric precursors of the 2021 Mw 7.1 Japan earthquake. Remote Sensing, 15(7), 1904. https://doi.org/10.3390/rs15071904

Eshkuvatov, H. E., Ahmedov, B. J., Tillayev, Y. A., Tariq, M. A., Shah, M. A., & Liu, L. (2023). Ionospheric precursors of strong earthquakes observed using six GNSS stations data during continuous five years (2011–2015). Geodesy and Geodynamics, 14(1), 65–79. https://doi.org/10.1016/j.geog.2022.04.002

Falayi, E. O., Adewole, A. T., Adelaja, A. D., Ogundile, A. A., & Roy-Layinde, T. O. (2020). Study of nonlinear time series and wavelet power spectrum analysis using solar wind parameters and geomagnetic indices. NRIAG Journal of Astronomy and Geophysics, 9(1), 226–237. https://doi.org/10.1080/20909977.2020.1728866

Habarulema, J. B., Yizengaw, E., Katamzi-Joseph, Z. T., Moldwin, M. B., & Buchert, S. C. (2018). Storm-time global observations of large-scale traveling ionospheric disturbances from ground-based and in situ satellite measurements. Journal of Geophysical Research: Space Physics, 123, 711–724.

Jonah, O. F., et al. (2020). Understanding interhemispheric traveling ionospheric disturbances and their mechanisms. Remote Sensing, 12(2), 228. https://doi.org/10.3390/rs12020228

Jonah, O. F., Kherani, E. A., & de Paula, E. R. (2016). Observation of TEC perturbation associated with medium-scale traveling ionospheric disturbance and a possible seeding mechanism of atmospheric gravity waves. Journal of Geophysical Research: Space Physics, 121, 2531–2546.

Kelley, M. C., Swartz, W. E., & Heki, K. (2017). Apparent ionospheric total electron content variations prior to major earthquakes due to electric fields created by tectonic stresses. Journal of Geophysical Research: Space Physics, 122(6), 6689–6695.

Kim, V. P., Hegai, V. V., & Illich-Svitych, P. V. (1994). On one possible ionospheric precursor of earthquakes. Physics of the Solid Earth, 30, 223–226.

Lizunov, G., Skorokhod, T., Hayakawa, M., & Korepanov, V. (2020). Formation of ionospheric precursors of earthquakes—Probable mechanism and its substantiation. Open Journal of Earthquake Research, 9(2), 142–169.

MacDougall, J. W., & Jayachandran, P. T. (2011). Spaced transmitter measurements of medium-scale traveling ionospheric disturbances near the equator. Geophysical Research Letters, 38, L16806.

Mikhailov, A. V., & Perrone, L. (2009). Pre-storm NmF2 enhancements at middle latitudes: Delusion or reality? Annales Geophysicae, 27(3), 1321–1330.

Namgaladze, A. A., Klimenko, M. V., Klimenko, V. V., & Zakharenkova, I. E. (2009). Physical mechanism and mathematical modeling of earthquake ionospheric precursors registered in total electron content. Geomagnetism and Aeronomy, 49(2), 252–262.

Patil, V., Atulkar, R., & Purohit, P. K. (2016). Analysis of ionospheric parameters above active seismic regions. Russian Journal of Earth Sciences, 16, ES1004.

Perrone, L., & Mikhailov, A. V. (2020). Daytime mid-latitude F2-layer quiet disturbances: A formation mechanism. Scientific Reports, 10, 9997.

Pulinets, S. A., et al. (2000). Quasi-electrostatic model of atmosphere–thermosphere–ionosphere coupling. Advances in Space Research, 26(8), 1209–1218.

Pulinets, S. A., & Boyarchuk, K. A. (2004). Ionospheric Precursors of Earthquakes. Springer.

Shah, M., et al. (2020). Possible ionosphere and atmosphere precursory analysis related to Mw > 6.0 earthquakes in Japan. Remote Sensing of Environment, 239, 111620.

Sugiura, M. (1963). Hourly values of equatorial Dst for the International Geophysical Year (IGY) (NASA Report X-611-63-131). NASA Goddard Space Flight Center.

Xu, T., et al. (2010). Abnormal perturbations in the ionospheric F2 region before the Wenchuan earthquake. Science China Earth Sciences, 53, 1671–1674.

Xu, T., et al. (2015). Is there any difference in local time variation in ionospheric F2-layer disturbances between earthquake-induced and quiet-disturbance events? Annales Geophysicae, 33, 687–695.

Xu, X., et al. (2022). Analysis of potential precursory patterns preceding two Mw ≥ 7 earthquakes in Mexico. Earth and Space Science, 9(10), e2022EA002267.

Yao, Y. B., et al. (2012). Analysis of ionospheric anomalies before the 2011 Mw 9.0 Japan earthquake. Chinese Science Bulletin, 57, 500–510.

Zolotov, O. V., Namgaladze, A. A., & Prokhorov, B. E. (2012). Total electron content disturbances prior to the 2011 Great Tohoku and 2011 Van earthquakes and their physical interpretation.

Zolotov, O. V., Namgaladze, A. A., Zakharenkova, I. E., Martynenko, O. V., & Shagimuratov, I. I. (2012). Physical interpretation and mathematical simulation of ionospheric precursors of earthquakes at mid-latitudes. Geomagnetism and Aeronomy, 52(3), 390–397.